Arch Med Vet 40, 161-168 (2008) DOI: 10.4067/s0301-732x2008000200008

ORIGINAL ARTICLE

Effects of artificially induced spinal cord compression on the canine cervical internal vertebral venous plexus: comparative evaluation of computed tomographic venography and digital subtraction venography

Efectos de la compresión de la médula espinal inducida artificialmente sobre el plexo venoso vertebral interno cervical en el perro: evaluación comparativa mediante venografía por tomografía computarizada y venografía por substracción digital

Gómez M,[a*] O Lanz[b], J Jones[b], R Broadstone[b], K Inzana[c], L Freeman[c]

[a]Instituto de Farmacología, Facultad de Ciencias Veterinarias, Universidad Austral de Chile, Valdivia, Chile.

[b]Department of Small Animal Clinical Sciences Virginia-Maryland Regional College of Veterinary Medicine, Virginia Polytechnic Institute & State University, Blacksburg, VA, USA.

[c]Department of Biomedical Sciences and Pathobiology, Virginia-Maryland Regional College of Veterinary Medicine, Virginia Polytechnic Institute & State University, Blacksburg, VA, USA.

RESUMEN

El plexo venoso vertebral interno (PVVI) es una red vascular localizada a lo largo del canal vertebral. El presente estudio fue diseñado para evaluar variaciones en la morfología del PVVI cervical bajo condiciones de compresión aguda de la médula espinal en perros. Una compresión medular experimental fue inducida en once perros adultos al nivel de C3/4 utilizando una técnica modificada de catéter de angioplastia con balón. Los perros fueron evaluados antes, durante y posterior a la compresión medular utilizando para ello venografía intraósea por substracción digital (VSD) y venografía por tomografía computarizada (TC). La VSD mostró pérdida manifiesta e inmediata de opacificación del PVVI cervical en el sitio de la compresión. La venografía por TC también evidenció pérdida de llenado del PVVI cervical con medio de contraste en las áreas comprimidas por el balón de angioplastia. La VSD también mostró cambios hemodinámicos del PVVI y sus ramas colaterales durante la compresión. Durante la postcompresión las imágenes de la VSD y la venografía por TC revelaron que algunos perros presentaban pérdida de llenado con medio de contraste del PVVI cervical en el área previamente comprimida. Los resultados de este estudio muestran que la compresión medular experimental en perros induce alteraciones locales inmediatas en la morfología venosa dentro del canal vertebral afectado.

Key words: spinal cord, computed tomography.

Palabras clave: compresión medular, tomografía computacional.

INTRODUCTION

The internal vertebral venous plexus (IVVP) is a network of valveless veins surrounding the vertebral canal, dura mater, spinal cord and spinal nerves (Evans 1993). Normal anatomy of the cervical internal vertebral venous plexus in dogs was described macroscopically (Worthman 1956, Reinhard *et al* 1962, Barone 1996) and by computed tomography (CT)(Gómez *et al* 2004). However, little is known about how acute spinal cord compression alters the IVVP morphology. Previous clinical studies in human beings suggest the IVVP may play a role in spinal cord injuries (Olmarker *et al* 1989, Delamarter *et al* 1990). In human beings (Groen and Ponssen 1990) and dogs, (Applewhite *et al* 1999) rupture of the IVVP was associated with spontaneous spinal epidural haematoma formation, leading to extradural compression of the spinal cord. Other abnormalities of the IVVP in human and veterinary patients include spontaneous congenital dilation of the cervical IVVP (Groen *et al* 2000, Hammer *et al* 2003) arteriovenous malformations (Hayashida *et al* 1999) and fibrocartilaginous embolism (Cauzinille 2000).

Based on a review of the literature, we theorized that the IVVP may play an important role in the pathophysiology of acute cervical spinal compression in dogs. Extradural compressive lesions (herniated disks, hematomas, neoplasms, and vertebral malformations) may cause congestion and/or collapse of vessels in this valveless venous system, which in turn may exacerbate or complicate cervical spinal cord and/or nerve root compression (Miyasaka *et al* 1978). Venous congestion and/or collapse may also extend beyond the site of compression and persist after surgical removal of the original inciting cause (Delamarter *et al* 1990).

The objectives of this study were to test the effects of acute cervical spinal cord compression on the morphology of the cervical IVVP in dogs, refine an experimental method for inducing acute cervical extradural compression and evaluate vertebral intraosseous DSV versus CT venography

Accepted: 31.07.2007.

* Casilla 567, Valdivia, Chile; marcelogomez@uach.cl

as techniques for demonstrating morphological changes in the IVVP caused by acute spinal compression in dogs.

Results of this study may explain the immediate effects of acute extradural compressive lesions on venous morphology in the cervical spine and improve the experimental compression and imaging techniques required for future studies of acute spinal cord compression in dogs.

MATERIAL AND METHODS

ANIMALS

Eleven adult Beagle dogs, weighing between 9 and 11 kg, were used in this study. Two dogs were used in pilot studies to standardize the experimental procedures and techniques. The remaining 9 dogs were tested using the protocols established during the pilot studies. All these animals were subjected to cervical spinal cord compression. Six dogs were used for digital subtraction venogram studies and 3 dogs for CT venographic studies. In all the 9 animals images were obtained during pre-compression, compression, and post-compression periods. All study protocols were approved by the Virginia Tech Institutional Animal Care and Use Committee.

ANAESTHESIA

The dogs were fasted for 12 hours prior to anaesthesia. Each dog was premedicated with butorphanol (0.2 mg/kg, IM), diazepam (0.2 mg/kg, IM), and atropine sulfate (0.02 mg/kg, IM). A 20-gauge over the needle catheter was placed in the cephalic vein and anaesthesia was induced by titrating 2% thiopental intravenously (13.6 ± 4.3 mg/kg, IV) at a dose just sufficient to allow tracheal intubation. Anaesthesia was maintained with isofluorane (1.1 to 1.2 %) in 100% O_2. Normal saline (0.9%) solution was administered IV at a rate of 10 ml/kg/hr. A 20-gauge over the needle catheter was then placed in a lingual artery for direct arterial blood-pressure measurement. Tidal volume and respiratory rate were controlled to maintain arterial eucapnia ($PaCO_2$, 35 to 45 mm Hg) using a volume-controlled ventilator.

EXPERIMENTAL SPINAL CORD COMPRESSION

This experimental model was a non-recovery surgical procedure. The spinal cord compression model used in our study was a modified technique initially described by Purdy *et al* (Purdy *et al* 2003, Purdy *et al* 2004). The lumbosacral space of each dog was clipped and aseptically prepared for angioplasty balloon catheter introduction. A 6 French introducer was percutaneously inserted into the lumbosacral space using fluoroscopic guidance, and a 145 cm Teflon coated guidewire (Cook Group Company, Bloomington, IN, USA) was then introduced and directed cranial to the cervical region. A 6 French angioplasty balloon catheter (Boston Scientific Corp., Flemont, CA, USA) (2 cm long and 6 mm diameter) was inserted over the guidewire until the radiopaque markers of the balloon were located between the third and fourth cervical vertebral bodies (figure 1). The guidewire was then removed. Following stabilization of physiologic parameters (mean arterial pressure, heart rate, respiratory rate, end tidal CO_2, O_2 saturation) in each dog, extradural spinal cord compression over caudal portion of C3 vertebral body, C3/4 intervertebral space level, and the cranial portion of C4 vertebral body was induced. Extradural compression was applied by rapid inflation of the balloon. Saline solution was injected manually through a syringe with an attached manometer until 4 atmospheres of pressure was achieved. This pressure allowed adequate balloon inflation. Balloon inflation was maintained for a period of 10 minutes.

DIGITAL SUBTRACTION VENOGRAPHY (DSV)

Digital subtraction venography combined with vertebral intraosseous injection of contrast medium was performed in 6 dogs. Three dogs were excluded due to insufficient opacification of the IVVP. Two of these 3 dogs had incomplete venograms of the cervical IVVP immediately after intraosseous injection of contrast medium in the C6 vertebral body. Three dogs exhibited sufficient opacification for inclusion in the experiment. For the 3 included dogs, digital subtraction venograms images were exposed for each treatment (pre-compression, compression and post-compression) using a digital fluoroscopic unit (Shimadzu Medical System, Torrance, CA, USA). After surgical preparation, a small skin incision was made in the left mid-cervical region. Using fluoroscopic guidance, a 13-gauge x 3.5 inches bone marrow biopsy/aspiration needle (Tyco Healthcare Group, Mansfield, MA, USA) was introduced manually into the vertebral body of the sixth cervical vertebra (C6). The position of the biopsy needle was checked in both dorso-ventral and lateral projections during introduction of the needle to ensure proper placement of the tip of the needle into the center of the vertebral body. The needle was flushed with heparinized saline solution to confirm proper needle placement. A syringe filled with 16 cc of contrast medium (meglumine iothalamate, 2 mg Iodine/kg) was connected to a 55 cm extension set and then attached to the bone biopsy needle. The extension set was used in order to reduce radiation exposure during manual injection. To facilitate intraosseous injection, contrast medium was pre-warmed to approximately 42˚C. Immediately before and during rapid injection of the contrast medium, dorso-ventral DSV images were acquired at a rate of 2 frames per second over a period of 10 seconds. The pre-compression venograms were performed following the placement of the angioplasty balloon catheter. Compression venograms were acquired following inflation of the angioplasty balloon catheter to a pressure of 4 atmospheres. Post-compression venograms were acquired following deflation of the balloon and after each dog's physiological parameters approached normal

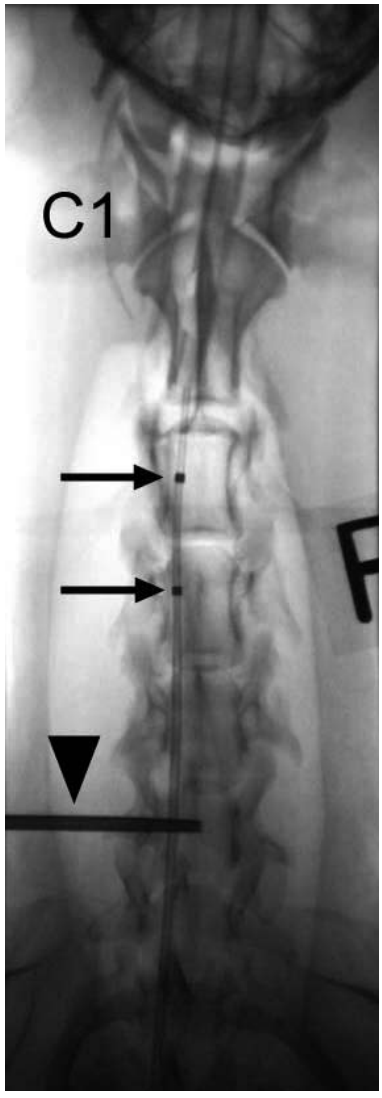

Figure 1. Dorso-ventral digital radiograph of the cervical region demonstrating the position of the angioplasty balloon catheter with its radiopaque markers (arrows) inside the C3/4 vertebral canal. The tip of the biopsy/aspiration needle is positioned within the vertebral body of C6 (arrowhead).

Radiografía digital dorsoventral de la región cervical que muestra la posición del catéter de angioplastia con sus marcadores radiopacos (flechas) dentro del canal vertebral de C3/4. La punta de la aguja de biopsia está posicionada dentro del cuerpo vertebral de C6 (cabeza de flecha).

values. This period was variable between dogs and it was approximately 10 minutes average. Each set of images was assigned a random identification number, and images were evaluated on a computer monitor using a window width of 1024 and a window level of 2048.

COMPUTED TOMOGRAPHY (CT)

Computed tomographic venography was performed in 3 dogs prior to compression, during compression and post-compression using the same compression and anaesthesia protocols as those used for the DSV dogs. Dogs were scanned using a helical CT scanner (Philips Medical Systems, Cleveland, OH, USA) and a standardized scanning protocol. Dogs were placed in sternal recumbency with the cervical spine extended and the thoracic and pelvic limbs were extended in a caudal direction. Lateral and dorsoventral pilot images were obtained to facilitate alignment of the neck and selection of slice locations. Precontrast CT scans were obtained using 3 mm slice thickness at 2 mm slice intervals, with a table pitch of 1.25. The scanned region extended from the external occipital protuberance to the spinous process of the first thoracic vertebra (T1) in all dogs. The CT gantry was angled as necessary to ensure slices were perpendicular to the vertebral canal. For CT venography images, scans were repeated after ionic contrast medium (Conray 400, Mallinkrodt Medical Inc., St Louis, MO, USA) which was intravenously administered through the previously placed lateral saphenous catheter. A manual bolus injection of 480 mg I/kg was administered at a rate of 2 ml/sec and spiral scanning was initiated immediately following bolus injection. Intravenous infusion of an additional 240 mg Iodine/kg of contrast medium was administered during the scan by means of a constant-rate infusion pump (Baxter Healthcare Corporation, Deerfield, IL, USA). During CT acquisition, mechanical ventilation was suspended to minimize breathing motion artifacts and to maximize filling of the cervical vertebral venous plexus.

DATA ANALYSIS

For the C1 to C7 vertebral levels, the following data were recorded from DSV and CT venograms:

- Presence of right and left components of the IVVP.
- Transverse diameters of the right and left IVVP at the mid-vertebral level and intervertebral space level.
- Distance between right and left components of the IVVP at the mid-vertebral level and intervertebral space level from C1 to C7.
- Presence of subjective abnormalities (occlusion, dilation, displacement or presence of collateral vessels) of the IVVP.

For measurements of the veins on DSV images, a calibration reference was used. The reference was defined as the distance between the 2 radiopaque markers of the angioplasty balloon catheter. These markers are known to be 2 cm apart and were located in the epidural space at the same geometric plane as the IVVP. This technique allowed correction for magnification effects produced in the DSV images.

Calculations of the parameters in the post-contrast CT images were made using a software for distance calculations. A window width of 300 HU and a window level of 100

HU were used during data measurements. Measurements of vein diameters from the DSV and post-contrast CT images were performed by a single observer.

Statistical significance between the differences in values of pre-compression, compression and post-compression in DSV and CT venograms were analyzed using a paired t test with a $P < 0.05$. Data analysis was performed using SAS statistical analysis system (SAS Institute Inc., Cary, NC, USA).

HISTOPATHOLOGICAL EXAMINATION

At the conclusion of the experimental studies, all dogs were euthanized by an intravenous overdose of sodium pentobarbital (390 mg/ml). For the 6 included dogs (3 DSV and 3 CT) with diagnostic imaging studies, the cervical spinal cord was removed from the vertebral canal, fixed in 10 % buffer formalin and embedded in paraffin. Samples were obtained from the following sites: the site of compression (spinal cord segment C3 and C4), cranial to the site of compression (spinal cord segment C2), caudal to the site of compression (spinal cord segment C8) and a site distant to compression (spinal cord segment L4). Serial transverse sections (4µm) were selected and stained with hematoxylin and eosin. Histological sections were evaluated by a board-certified veterinary pathologist.

RESULTS

DIGITAL SUBTRACTION VENOGRAPHY (DSV)

Evaluation of the vertebral venous plexus was successful in 3 of 6 dogs in which DSV was performed. Vascular anatomy pattern of the cervical IVVP during pre-compression was consistent between the 3 dogs. The DSV images clearly depicted symmetrical right and left components of the IVVP and the intervertebral veins (figure 2). Intervertebral veins located between C2/3, C3/4, C4/5 and C5/6 vertebral levels were represented by double vessels, visible on both sides of the cervical vertebral canal (figure 2). The vertebral veins were also identified on both sides of the vertebral canal, communicating with the IVVP via the intervertebral veins (figure 2). Transverse diameters of the IVVP ranged from 1.72 mm to 3.2 mm, with a mean of 2.54 ± 0.29 mm for the right IVVP and 2.59 ± 0.45 mm for the left IVVP.

During compression, the cervical IVVP appeared optimal for evaluation at frame 12 of the total 20 frames of the DSV. Transverse diameter of the left IVVP on the compression images had significantly lower values between the segments of C3 to C5 compared with pre-compression images. The mean transverse diameter of the IVVP for this region (C3-C5) was 1.25 ± 0.62 mm. Compression DSV images in all 3 dogs showed total or partial lack of filling with contrast medium of IVVP in areas of compression and segments adjacent to it (figure 3).

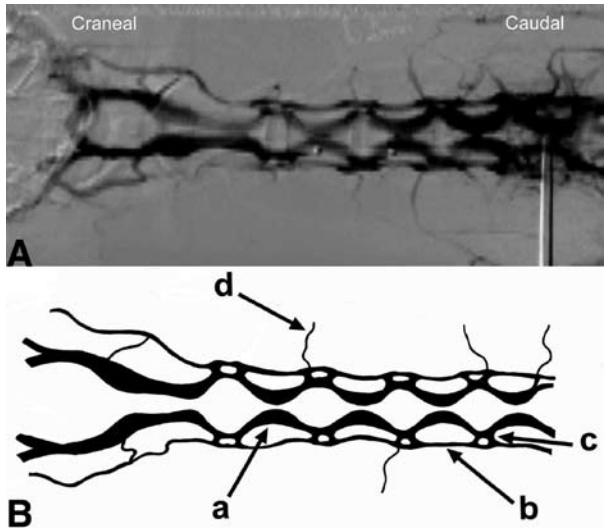

Figure 2. Pre-compression digital subtraction venogram (A) and diagram (B) of the IVVP in the cervical region of a dog. Notice the symmetrical and undulating appearance of the cervical internal vertebral venous plexus. Internal vertebral venous plexus (a), vertebral vein (b), intervertebral vein (c), muscular branches (d).

Venograma por substracción digital precompresivo (A) y diagrama (B) del PVVI en la región cervical del perro. Nótese la apariencia simétrica y undulante del plexo venoso vertebral interno a nivel cervical. Plexo venoso vertebral interno (a), vena vertebral (b), vena intervertebral (c), ramas musculares (d).

Mean values of transverse diameters of the IVVP between C3 and C5 during post-compression were 1.75 ± 0.4 mm for the left side and 1.55 ± 0.4 mm for the right side. Both diameter values were lower than pre-compression values but higher than compression values.

COMPUTED TOMOGRAPHY

Evaluation of the postcontrast CT compression images revealed adequate visualization of the veins of the cervical vertebral canal in 2 of the 3 dogs. One problem in the images was the presence of hypoattenuating areas (-764 Hounsfield units) in the epidural space between C4-C7 in 2 dogs. These areas were produced most likely due to epidural air introduced during catheter placement. However, evaluation of the IVVP in the remaining cervical vertebral segments was possible in all dogs (figure 4A). Mean transverse diameters of the IVVP for C1 to C7 in pre-compression CT venograms were 3.2 ± 0.98 mm for the right IVVP and 2.93 ± 1.39 mm for the left IVVP. The maximal transverse diameter of the IVVP was observed at C6 with a mean of 4.42 ± 0.20 mm for the right and left IVVP. The minimal transverse diameter of the IVVP during pre-compression was observed at C1 with a mean of 1.91 ± 0.39 mm for both components of the IVVP. The distance between medial borders of the IVVP was maximal over the atlas with 10.56 ± 1.12 mm between the right and left IVVP.

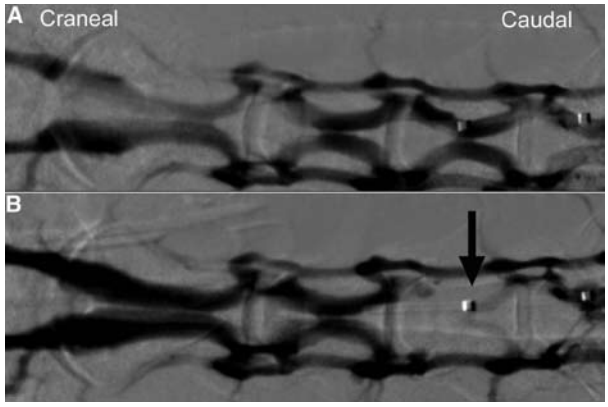

Figure 3. Magnified pre-compression (A) and compression (B) digital subtraction venograms of the cranial cervical region obtained from the same dog. Notice the bilateral lack of filling of the internal vertebral venous plexus in the area of compression (arrow) on image B.

Venogramas por substracción digital durante la precompresión (A) y compresión (B) magnificados. Nótese el defecto de llenado del plexo venoso vertebral interno en el área de la compresión (flecha) en la imagen B.

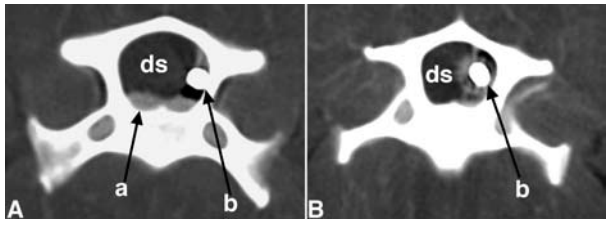

Figure 4. Pre-compression transverse CT venographic image at the mid-portion of C5 (A). Transverse CT venographic image at C4 during compression (B). Internal vertebral venous plexus (a), angioplasty balloon catheter in the epidural space in A (b), and dural sac (ds). Notice in image 4B the right ventrolateral displacement of the dural sac, and the lack of filling of the internal vertebral venous plexus.

Imagen transversal por venografia TC durante la precompresión a nivel de la porción media de C5 (A). Imagen transversal por venografía TC durante la compresión (B). Imagen de venografía TC durante la precompresión a nivel medio de C5 (A). Imagen de venografía TC durante la compresión a nivel de C4 (B). Plexo venoso vertebral interno (a), catéter con balón de angioplastia en el espacio epidural en A (b), y saco dural (ds). Nótese el desplazamiento ventrolateral derecho del saco dural y la pérdida de llenado del plexo venoso vertebral interno en la imagen 4B.

Computed tomographic venography images during compression showed no opacification of the right and left IVVP between C3-C5 vertebral levels in all 3 dogs (figure 4B). Measurements of transverse diameter of IVVP (mean: 3.16 ± 0.93 mm for left component and 3.6 ± 1.06 mm for right component) and distance (mean: 7.45 ± 1.48 mm at intervertebral level and 1 mm over the vertebral bodies) between right and left components of the IVVP during compression at C1, C1/2, C2 and C2-C3 vertebral segments were similar to pre-compression CT venography values. The transverse diameters values between C5 and C7 in one dog were also similar to pre-compression values in the 3 dogs with a mean diameter of 4.32 ± 0.28 mm. In the other 2 dogs, gas in the epidural space compressed the IVVP.

Post-compression CT venography images did not demonstrate the IVVP between C3 and C4-C5 vertebral segments. Presence of epidural air within the C6 and C7 vertebral canal in 2 dogs made it difficult to visualize the IVVP on post-compression CT venography images.

HISTOLOGICAL EXAMINATION

In all 6 dogs (3 DSV and 3 CT venography), spinal cord examination from the areas in direct contact with the angioplasty balloon catheter during compression were consistent with acute spinal cord trauma. In 5 of the transversely sectioned specimens revealed a central hemorrhagic core on gross examination (figure 5). Under microscopic examination, 3 dogs had spinal cord samples with central tissue disruption, and cavitary lesions in the gray matter with multiple areas of adjacent recent perivascular hemorrhage. Hemorrhage was principally located in the dorsal horn and central intermediate substance that surrounds the central canal. The remaining 3 dogs showed unilateral and bilateral areas of recent perivascular hemorrhage. No abnormalities were observed in the L4 spinal cord samples.

DATA ANALYSIS

Measured values of vein diameters were compared between treatments (pre-compression, compression, and post-compression) in the DSV group and the CT venography group. Significant differences in the transverse diameters were found between pre-compression and compression in the left IVVP at the C3 vertebral level (P= 0.048). Also, the transverse diameter of the right IVVP at the C3/4 vertebral level differed (P = 0.033) between pre-compression and post-compression treatments.

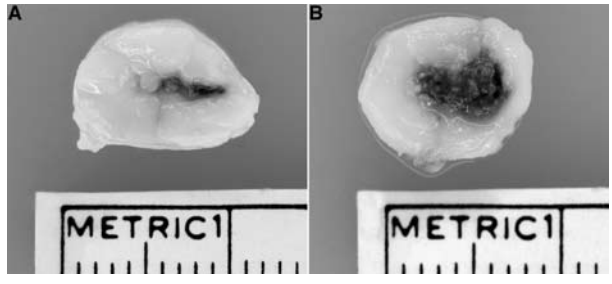

Figure 5. Transverse views of compressed spinal cord sections obtained at C4 (A) and C5 (B) spinal cord segments from 2 dogs. Notice the central area of haemorrhage in both cases.

Vistas transversales de secciones de médula espinal sometidas a compresión a nivel de los segmentos medulares C4(A) y C5 (B). Nótese el área central de hemorragia en ambos casos.

DISCUSSION

The spinal compression technique used in this study produced consistent spinal cord compression in all 6 included dogs. This technique was modified from previously described methods (Purdy *et al* 2003, Purdy *et al* 2004). The previous models consisted of a subarachnoid introduction of the angioplasty balloon catheter by a lateral lumbar foraminal approach instead of the lumbosacral and epidural approach used in our study. The balloon model in both cases provided the advantage of avoiding an invasive surgical procedure such as a laminectomy (Schwartz and Himes 2003). Laminectomy could significantly alter the haemodynamics of the IVVP, especially in the post compression period (Doppman 1976).

The model used in this study created similar histopathological changes to those seen in previous reports of dogs and human beings with acute spinal cord compression (Norenberg *et al* 2004). Areas of perivascular hemorrhage and cavitary lesions, mainly in the gray matter, were identified. Central haemorrhage is believed to be due to rupture of post-capillary venules and sulcal arterioles, by either mechanical disruption directly from trauma, or from intravascular coagulation leading to venous stasis and distention (Tator and Koyanagi 1997). Studies indicate that the degree of compression (balloon inflation) seems to be more important than the duration of compression in determining the severity of spinal cord damage (Purdy *et al* 2004). However, in a clinical setting, spinal cord compression lesions are many times more complex and their duplication in experimental studies is impossible (Hitchon *et al* 1990).

DIGITAL SUBTRACTION VENOGRAPHY

Our results showed that the morphology of the cervical IVVP on pre-compression DSV images was in accordance with anatomical descriptions from the literature (Worthman 1956, Reinhard *et al* 1962, Evans 1993, Barone 1996). Pre-compression DSV sequences also clearly demonstrated the anastomoses of the cervical IVVP with the intervertebral veins, vertebral veins, and cerebral veins.

The current study indicates that DSV imaging characteristics and some dimensions of the cervical IVVP were affected by acute, experimental, extradural compression of the cervical spinal cord. Digital subtraction venography images showed regions of complete or partial lack of filling of the IVVP in areas associated with balloon compression. Previous studies in monkeys, using conventional venography and a similar balloon compression model in the lumbar region, also demonstrated total obstruction of the IVVP during balloon inflation (Doppman 1976). Intraosseous and catheter epidural venography in human beings and dogs have been reported to display unilateral or bilateral block of the IVVP at the site of disk herniation (LePage 1974, Theron 1976, Miyasaka *et al* 1978, Blevins 1980). Venographic studies in human beings have also demonstrated that, in cases of cervical disk disease, interruption of the IVVP usually occurs at multiple vertebral levels (Miyasaka *et al* 1978). Apparently, this multiple IVVP interruption pattern is observed more often than a single pattern. In human patients with intermittent claudication, magnetic resonance phlebography has shown areas of extensive filling defects of the IVVP at the lumbosacral region (Manaka *et al* 2003).

During compression, veins easily collapse due to their low internal pressure and wall laxity (Kaiser *et al* 1984). Extradural compression induces a rapid increase of epidural pressure. Wolfla *et al* (2004) indicated that ventral cervical epidural pressure increases sharply when an epidural mass occupies more than 20% of the cervical vertebral canal space. According to our data, we calculated that our experimental model compromised more than 40% of the vertebral canal over C3 and C4 vertebral bodies. Therefore, our model applies considerable pressure on cervical vertebral canal components.

During compression, left to right distance between the components of the IVVP did not differ compared with pre-compression or post-compression values. However, spinal conditions such as central protruded disk material or neoplastic masses inside the vertebral canal can increase the distance between IVVP components (Miyasaka *et al* 1978). The increase in distance between IVVP components was not observed in our dogs. This was probably caused by our lateral positioning of the angioplasty balloon catheter in the vertebral canal.

Our DSV findings during compression demonstrated increases in transverse diameters of the IVVP in areas immediately cranial or caudal to the spinal cord compression. Those values were not statistically significant. Magnetic resonance imaging studies in human beings have demonstrated that spinal compression from masses produce IVVP congestion (Morikawa *et al* 1996). The venous congestion is due to blood accumulation in the venous sinuses cranial to the site of compression (Zimmerman *et al* 1994). We did observe some congestion of the IVVP during compression as a result of increased density of vessels cranial to the area of compression. However we did not observe increased diameter of the vessels. The most likely reason for this is that we only applied compression for 10 minutes and perhaps a longer period of experimental spinal cord compression may be needed to cause a distinctive venous congestion adjacent to the site of compression.

Post-compression DSV images of the cervical IVVP were variable. One dog had no change in IVVP morphology and 2 dogs had complete lack of opacification of the IVVP at the site of compression. This late and persistent lack of filling of the IVVP may have been due to spinal cord swelling following compression that constricted the IVVP. Similar observations were found by Doppman (1976) who observed obstruction of the lumbar IVVP

in primates, 4 hours after experimental spinal cord compression. In human beings with disk herniation or spinal neoplasia, long standing compression of the IVVP may result in irreversible occlusion of the venous plexus at the affected site, despite successful spinal cord decompression (Miyasaka *et al* 1978, Kato 1985). Venous stasis produced during spinal cord compression may lead to white matter oedema that subsequently exacerbates the spinal cord secondary damage and IVVP compression (Kato 1985, Olmarker *et al* 1989, Tator and Koyanagi 1997). Vasoactive agents (norepinephrine, serotonin, prostaglandin), known to be released during acute spinal cord compression, may also contribute to the persistent vertebral venoconstriction observed on post-compression DSV images (Osterholm and Mathews 1972). Post-traumatic changes in the IVVP due to introduction of the angioplasty balloon catheter may also cause interference in the IVVP circulation and contribute to the post-compression venous collapse.

A consistent DSV finding was that external jugular veins were filled with contrast medium in earlier frames of compression and post-compression DSV studies (frame 11) compared to pre-compression DSV studies (frame 16 through 20). In one animal the internal jugular vein was seen clearly during compression, but not during pre-compression and post-compression. These observations indicate that compression or factors associated with compression may produce alterations in haemodynamics of the IVVP and increase shunting of blood into communicating veins. Several authors have found that individuals with spinal cord injury presented with abnormal systemic venous circulation (Chantraine *et al* 1979, Cassar-Pullicino *et al* 1995). Various factors are proposed for these altered venous hemodynamics findings. Spinal cord injury (SCI) can induce autonomic dysfunction that may alter the passive resistance of veins and promote changes in the IVVP flow (Chantraine *et al* 1979). Changes in intra-abdominal pressure, associated with altered diaphragmatic and abdominal muscle function after SCI may also affect the caval and vertebral venous system flow (Epstein *et al* 1970, Cassar-Pullicino *et al* 1995).

COMPUTED TOMOGRAPHIC VENOGRAPHY

Non-selective CT venography evaluation of the cervical IVVP was performed in 3 dogs during pre-compression, compression, and post-compression. The imaging protocol developed in our study was less invasive than intraosseous DSV, and more consistently resulted in adequate opacification of the venous structures located inside the cervical vertebral canal. Similar results were obtained in a non selective venographic CT study performed in the cervical region in adult dogs (Gomez *et al* 2005). The two major limitations of the technique were the presence of epidural gas in the epidural space in 2 dogs, and the presence of small streak artifacts produced by the radiopaque markers inside the vertebral canal. Another limitation of the CT venography technique compared with DSV was the inability to measure changes in IVVP flow dynamics for each treatment.

As in DSV, CT venography was able to demonstrate filling defects of the IVVP during experimental spinal cord compression. In 2 cases, CT venography showed displacement of the spinal cord in a direction opposite to the site of compression; therefore, obliterating the contralateral IVVP. In two of the 3 CT venograms, air bubbles located in the ventral and lateral epidural space of the caudal cervical region were observed. These air filled bubbles adopted the contour of the epidural space and were able to compress the vertebral venous plexus. Air collection in the epidural space is reported to be an incidental finding, usually with no clinical importance (Hjarbaek *et al* 1992).

Our study had some limitations. The data obtained from this study was not intended to describe DSV or CT venographic findings on IVVP morphology in all cases of acute spinal cord compression. This was a rather exploratory study designed to evaluate a spinal cord compression model and compare two imaging techniques. Reports suggest agreement between CT angiography and digital subtraction angiography are very high ($r > 90\%$) for evaluation of vascular components (Link *et al* 1996, Kaatee *et al* 1997). Despite the relative small study population, DSV and CT venography consistently demonstrated changes in IVVP morphology during experimental spinal cord compression. However, CT venography offers a better evaluation than DSV of dimensions, morphology and relations of the IVVP with the other neighbouring structures in the vertebral canal.

Additionally, the spinal cord compression model used in our study represented a simple model for creating acute spinal cord compression in dogs. This experimental model has several advantages. First, it provides an easy method to change the selected site of spinal cord compression. Under fluoroscopic guidance, the guidewire can be directed cranially or caudally without problems, facilitating placement of the angioplasty balloon catheter over the desired vertebral canal location. Second, radiopaque markers of the angioplasty balloon catheter are recognized on DSV images and can be used as reference objects if measurements are required. Finally, the model is minimally invasive, and produced consistent spinal cord lesions.

In conclusion, our study demonstrates early alterations in cervical vertebral venous plexus morphology under experimental spinal cord compression in dogs. These variations in venous morphology were detected using digital subtraction venography and CT venography. The study also showed that the spinal cord compression model used in our study represents a consistent and reliable method for studying acute spinal cord compression in dogs. Further studies are needed to evaluate specific hemodynamic changes of the canine cervical IVVP under acute spinal cord compression conditions.

SUMMARY

The internal vertebral venous plexus (IVVP) is a vascular network located along the vertebral canal. The present study was designed to assess variation in morphology of the cervical IVVP under experimental acute spinal cord compression in dogs. Experimental spinal cord compression was induced in 9 adult dogs at C3/4 vertebral canal level using a modified angioplasty balloon catheter technique. Dogs were evaluated prior to, during and post spinal cord compression using vertebral intraosseous digital subtraction venography (DSV) and computed tomographic (CT) venography. DSV demonstrated significant and immediate lack of opacification of the cervical IVVP at the site of compression. CT venography also demonstrated a similar lack of filling of the IVVP in areas of balloon compression. DSV images demonstrated the hemodynamic changes of the IVVP and their collateral veins during compression. During post-compression, DSV and CT venography images revealed that 5 dogs exhibited lack of filling of the cervical IVVP at the previously compressed area. Findings show that experimental spinal cord compression induces immediate local venous morphological alteration at the involved vertebral canal area.

REFERENCES

Applewhite AA, BE Wilkens, DE McDonald, RM Radasch, RD Barstad. 1999. Potential central nervous system complications of von Willebrand's disease. *J Am Anim Hosp Assoc* 35, 423-429.

Barone R. 1996. *Anatomie Comparee des Mammiferes Domestiques*. Tome 5. Angiologie, Vigot, Paris, France.

Blevins E. 1980. Transosseous vertebral venography: A diagnostic aid in lumbosacral disease. *Vet Radiol* 21, 50-54.

Cassar-Pullicino VN, E Colhoun, M McLelland, IW McCall, W el Masry. 1995. Hemodynamic alterations in the paravertebral venous plexus after spinal injury. *Radiology* 197, 659-663.

Cauzinille L. 2000. Fibrocartilaginous embolism in dogs. *Vet Clin North Am Small Anim Pract* 30, 155-167.

Chantraine A, C van Ouwenaller, HJ Hachen, P Schinas. 1979. Intramedullary pressure and intra-osseous phlebography in paraplegia. *Paraplegia* 17, 391-399.

Delamarter RB, HH Bohlman, LD Dodge, C Biro. 1990. Experimental lumbar spinal stenosis. Analysis of the cortical evoked potentials, microvasculature, and histopathology. *J Bone Joint Surg Am* 72, 110-120.

Doppman JL. 1976. Angiographic changes following acute spinal cord compression: an experimental study in monkeys. *Br J Radiol* 49, 398-406.

Epstein HM, HW Linde, AR Crampton, IS Ciric, JE Eckenhoff. 1970. The vertebral venous plexus as a major cerebral venous outflow tract. *Anesthesiology* 32, 332-337.

Evans H. 1993. Veins. In: Evans H (ed). *Miller's anatomy of the dog*. 3rd ed. WB Saunders, Philadelphia, USA, Pp 682-716.

Gómez M, L Freeman, J Jones, O Lanz, P Arnold. 2004. Computed tomographic anatomy of the canine cervical vertebral venous system. *Vet Radiol Ultrasound* 45, 29-37.

Groen RJ, DA Batchelor, PV Hoogland. 2000. Congenital dilatation of the cervical epidural venous plexus: neuroradiology and endovenous management. *Minim Invasive Neurosurg* 43, 109-110.

Groen RJ, H Ponssen. 1990. The spontaneous spinal epidural hematoma. A study of the etiology. *J Neurol Sci* 98, 121-138.

Hammer A, I Knight, A Agarwal. 2003. Localized venous plexi in the spine simulating prolapse of an intervertebral disc: a report of six cases. *Spine* 28, E5-E12.

Hayashida E, K Ochiai, T Kadosawa, T Kimura, T Umemura. 1999. Arteriovenous malformation of the cervical spinal cord in a dog. *J Comp Pathol* 121, 71-76.

Hitchon PW, GN Dyste, RK Osenbach, MM Todd, T Yamada, AE Jensen. 1990. Spinal cord blood flow in response to focal compression. *J Spinal Disord* 3, 210-219.

Hjarbaek J, PW Kristensen, P Hauge. 1992. Spinal gas collection demonstrated at CT. *Acta Radiol* 33, 93-96.

Kaatee R, FJ Beek , EE de Lange, MS van Leeuwen, HF Smits, PJ van der Ven, JJ Beutler, WP Mali. 1997. Renal artery stenosis: detection and quantification with spiral CT angiography versus optimized digital subtraction angiography. *Radiology* 205,121-127.

Kaiser MC, P Capesius, A Roilgen, G Sandt, D Poos, G Gratia. 1984. Epidural venous stasis in spinal stenosis. CT appearance. *Neuroradiology* 26, 435-438.

Kato A. 1985. Disturbance of the circulation in the spinal cord with epidural neoplasm. *Med J Osaka* 35, 63-71.

LePage JR. 1974. Transfemoral ascending lumbar catheterization of the epidural veins. Exposition and technique. *Radiology* 111, 337-339.

Link J, S Muller-Hulsbeck, F Wesner, JC Steffens, J Brossmann, M Heller. 1996. Spiral CT angiography versus DSA in detection of carotid stenoses. *Zentralbl Chir* 121, 1018-1022.

Manaka M, M Komagata, K Endo, A Imakiire. 2003. Assessment of lumbar spinal canal stenosis by magnetic resonance phlebography. *J Orthop Sci* 8, 1-7.

Miyasaka K, H Takei, T Ito, K Tashiro, H Abe, M Tsuru. 1978. Catheter cervical vertebral venography. *Neuroradiology* 16, 413-415.

Morikawa M, S Sato, Y Numaguchi, F Mihara , MI Rothman. 1996. Spinal epidural venous plexus: its MR enhancement patterns and their clinical significance. *Radiat Med* 14, 221-227.

Norenberg MD, J Smith, A Marcillo. 2004. The pathology of human spinal cord injury: defining the problems. *J Neurotrauma* 21, 429-440.

Olmarker K, B Rydevik, S Holm, U Bagge. 1989. Effects of experimental graded compression on blood flow in spinal nerve roots. A vital microscopic study on the porcine cauda equina. *J Orthop Res* 7, 817-823.

Osterholm JL, GJ Mathews. 1972. Altered norepinephrine metabolism following experimental spinal cord injury. 1. Relationship to hemorrhagic necrosis and post-wounding neurological deficits. *J Neurosurg* 36, 386-394.

Purdy PD, RT Duong, CL White, DL Baer, RR Reichard, GL Pride Jr., C Adams, S Miller, CL Hladik , Z Yetkin. 2003. Percutaneous translumbar spinal cord compression injury in a dog model that uses angioplasty balloons: MR imaging and histopathologic findings. *Am J Neuroradiol* 24, 177-184.

Purdy PD, CL White, DL Baer, WH Frawley, RR Reichard, GL Pride, C Adams, S Miller, CL Hladik, Z Yetkin. 2004. Percutaneous translumbar spinal cord compression injury in dogs from an angioplasty balloon: MR and histopathologic changes with balloon sizes and compression times. *Am J Neuroradiol* 25, 1435-1442.

Reinhard KR, ME Miller, HE Evans. 1962. The craniovertebral veins and sinuses of the dog. *Am J Anat* 111, 67-87.

Schwartz ED, BT Himes. 2003. New model of minimally invasive experimental spinal cord injury. *Am J Neuroradiol* 24, 166-168.

Tator CH, I Koyanagi. 1997. Vascular mechanisms in the pathophysiology of human spinal cord injury. *J Neurosurg* 86, 483-492.

Theron J. 1976. Cervicovertebral phlebography: pathological results. *Radiology* 118, 73-81.

Wolfla CE, BE Snell, JH Honeycutt. 2004. Cervical ventral epidural pressure response to graded spinal canal compromise and spinal motion. *Spine* 29, 1524-1529.

Worthman RP. 1956. The longitudinal vertebral venous sinuses of the dog. I. Anatomy. *Am J Vet Res* 17, 341-348.

Zimmerman GA, K Weingarten, MH Lavyne. 1994. Symptomatic lumbar epidural varices. Report of two cases. *J Neurosurg* 80, 914-918.